Divergence of a Propulsive Plasma Flow Expanding through a Magnetic Nozzle

IEPC-2009-260

Justin M. Little[*] and Edgar Y. Choueiri[†]
Princeton University, Princeton, NJ, 08544, USA

An analytical expression for the divergence angle of an energetic plasma exhaust plume emerging from a solenoidal magnetic nozzle is derived in the context of the ideal magneto-hydrodynamics detachment scenario. This detachment scenario assumes that the plasma flow effectively stretches the magnetic field lines to infinity as the kinetic energy density of the plasma exceeds the energy density stored within the magnetic field. A coordinate transformation of the ideal magnetohydrodynamics equations for a cold plasma reveals an expression for the divergence angle with respect to both the ratio of the incoming flow energy density to the magnetic field energy density at the nozzle throat (β_0) and the ratio of the incoming plasma radius to the radius of the nozzle ($\bar{r}_{p0}$). The divergence angle is found to significantly decrease for increasing values of β_0 until the point where $\beta_0 \simeq 0.12\bar{r}_{p0}^{1/2}$. After this point, only marginal divergence angle increases are possible. A comparison of the cold-plasma divergence angle expression with experimental evidence reveals that thermal expansion effects are not negligible.

Nomenclature

β = ratio of plasma flow energy density to magnetic field energy density
β_0 = β at nozzle entrance
$\boldsymbol{B}$ = magnetic field vector
$\bar{\boldsymbol{B}}$ = normalized magnetic field vector
$\bar{\kappa}_0$ = normalized magnetic field line curvature at the nozzle throat
dt = time step
$d\tau$ = dimensionless time step
μ_0 = permeability of free space
η = nozzle efficiency
Φ = flux surface label
Φ_p = flux surface label corresponding to the plasma edge
$\bar{\mathcal{R}}_0$ = radius of curvature of the magnetic field line at the nozzle throat
r_c = radius of nozzle coils
r_{p0} = radius of plasma at nozzle entrance
ρ = plasma mass density
ρ_0 = plasma mass density at nozzle entrance
$\bar{\rho}$ = dimensionless plasma mass density

---

[*]Graduate Student, Mechanical and Aerospace Engineering, jml@princeton.edu.
[†]Professor, Mechanical and Aerospace Engineering, choueiri@princeton.edu.

θ	=	angle between solenoid axis and magnetic field vector
θ_p	=	θ along the plasma edge
θ_p^*	=	initial θ along the plasma edge
θ_{div}	=	divergence angle of plume
τ	=	dimensionless time
u_0	=	plasma velocity at the nozzle throat
$\boldsymbol{u}$	=	plasma velocity vector
$\bar{\boldsymbol{u}}$	=	normalized plasma velocity vector
$u_\perp$	=	plasma velocity perpendicular to magnetic field line
$\bar{u}_\perp$	=	normalized plasma velocity perpendicular to magnetic field line
$\bar{z}$	=	dimensionless axial distance
$\bar{r}$	=	dimensionless radial distance
$\bar{r}_{p0}$	=	radius of the plasma normalized by the coil radius

I.   Introduction

MAGNETIC nozzles typically use a converging-diverging magnetic field to convert the thermal energy of a plasma into directed kinetic energy while simultaneously preventing the energetic plasma from impacting the physical walls. Recent advances in efficient plasma heating using radio frequency waves have renewed interest in magnetic nozzles for plasma propulsion applications in space.[1,2] Magnetic nozzles are a desirable acceleration mechanism for thermal plasmas because they do not require the use of electrodes, which frequently limit the performance and usable lifetime of electric thrusters. The feasibility of using solenoidal magnetic fields as a mechanism to produce thrust has been questioned, however, due to the tendency of plasma to remain tied to necessarily closed magnetic field lines.[3] A physical mechanism is thus required to detach the plasma from the spacecraft's magnetic field with minimal plume divergence if thrust is to be achieved in an efficient manner.

As a consequence of their unknown capacity for thrust generation, the focal point of recent magnetic nozzle research has been the issue of plasma detachment.[4−7] Initially, it was widely believed that resistive diffusion of particles across magnetic field lines would be the predominant mechanism for detachment.[4] However, detachment through resistive diffusion provided a bleak outlook for magnetic nozzles for plasma propulsion applications as the plume region is typically characterized by low resistivity. Alternatively, Hooper showed that cross-field transport and detachment occur for a two-fluid plasma flowing through a static dipole field due to ambipolar drift motion.[5] Hooper's analysis ultimately concluded that plasma detachment from magnetic nozzles would be a very inefficient process as only a small fraction of the exhaust would be converted into directed flow along the thrust axis. Building upon Hooper's model, Schmit and Fisch demonstrated that the detachment efficiency of a magnetic nozzle can be significantly increased if unique angular velocity profiles can be induced within each species near the nozzle entrance.[6] Recently, Arefiev and Breizman proposed that, in the context of ideal MHD theory, plasma detachment may occur as the kinetic energy density of the propulsive plasma exceeds the energy density stored within the magnetic field of the nozzle.[7] They suggest that beyond this point, the plasma stretches the magnetic field lines along with the flow in a process similar to the solar wind (see figure 1).

Although a rigorous analytical proof of the "frozen-in" detachment scenario of Arefiev and Breizman has yet to be formulated, computer simulations[8−10] and experimental measurements[11−12] have been employed to verify the theory. In an extension of the original analytic model, Breizman et al. used a Lagrangian code to show that the steady-state motion of the plasma plume is not tied to the vacuum magnetic field lines of the nozzle.[8] Furthermore, Winglee et al. managed to show the time-evolved stretching of the magnetic field within the exhaust plume along the thrust axis using three-dimensional multifluid simulations.[9] A similar effect is also shown using both MHD and particle-in-cell (PIC) simulations by Ilin et al.[10] Experimentally, Deline et al. measured a noticeable deviation from vacuum-field-aligned flow at the point when the flow energy density becomes comparable to the magnetic field energy density.[11] However, measurements of the field evolution in the same experiment could not coincide this result with magnetic field stretching.[12]

Assuming "frozen-in" detachment does occur, the question of the efficiency of the process arises. In that context, the angle at which the plasma detaches from the spacecraft's magnetic field heavily influences the

efficiency of the thruster because flow divergence decreases the momentum exchange along the thrust axis. Previous studies have focused on the ability of a plasma to detach from a magnetic nozzle and have not addressed the dependence of the flow's divergence angle on the initial flow conditions.[7,8] Furthermore, these studies employed a "paraxial approximation," which assumes the radial component of the magnetic field is much less than the axial component, thus limiting their accuracy within the exhaust plume where the magnetic field components become comparable.

In this study we investigate the divergence of a non-paraxial propulsive plasma flow from a solenoidal magnetic nozzle assuming the magnetic field evolution within the plume acts according to the "frozen-in" detachment scenario (fig. 1). In particular, we seek an expression that gives the flow's divergence angle as a function of the initial flow conditions at the nozzle's throat.

For that goal, we start with a coordinate transformation that recasts the magnetic induction equation in terms of the magnetic field strength and orientation with respect to the nozzle axis. Using scaling relations based on the ideal MHD equations, we solve a differential equation describing the time-evolution of the field orientation in the far-field exhaust plume. The limit of this solution as time goes to infinity yields the divergence angle of the plume as a function of the initial plasma radius and the ratio of the plasma kinetic energy to magnetic field energy density at the nozzle throat. Finally, we discuss the physical implications of the divergence angle expression and compare its results to previous computational and experimental findings.
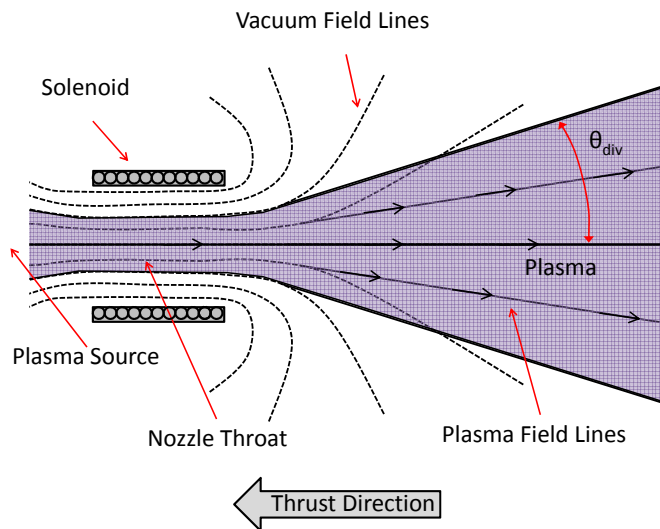

Figure 1. Illustration describing the "frozen-in" detachment scenario in which an energetic plasma effectively drags the magnetic field lines of a magnetic nozzle to infinity. The vacuum field lines are shown as dotted lines and those in the presence of the plasma flow are shown as solid lines. The half-angle at which the plume detaches, is denoted as θ_{div}.

II.   Problem Description

The evolution of both the velocity and magnetic field within a magnetic nozzle plume is highly complex due to many factors. Induced currents affect the magnetic field structure of the plasma, which in turn affects the dynamics of the plasma and the current distribution itself. Resistivity of the plasma leads to diffusion of the magnetic field across the vacuum-plasma interface, thus further complicating the already rich set of time-evolving boundary conditions. Furthermore, a competition exists between the adiabatic expansion of the plasma and the expansion due to the magnetic field. In order to simplify the problem and isolate the physics of magnetic field evolution, we start off by assuming the plume may be described as an infinitely conducting, cold plasma. Thus, the problem may be cast in the context of ideal MHD theory.

A. Ideal Magnetohydrodynamics

The time-dependent ideal MHD equations for a cold plasma may be written as:[13]

$$\rho \frac{\partial \boldsymbol{u}}{\partial t} + \rho \left(\boldsymbol{u} \cdot \boldsymbol{\nabla} \right) \vec{u} = -\frac{1}{\mu_0} \boldsymbol{B} \times \left(\boldsymbol{\nabla} \times \boldsymbol{B} \right), \tag{1}$$

$$\frac{\partial \rho}{\partial t} + \boldsymbol{\nabla} \cdot \left(\rho \boldsymbol{u} \right) = 0, \tag{2}$$

$$\frac{\partial \boldsymbol{B}}{\partial t} = \boldsymbol{\nabla} \times \left(\boldsymbol{u} \times \boldsymbol{B} \right), \tag{3}$$

$$\boldsymbol{\nabla} \cdot \boldsymbol{B} = 0. \tag{4}$$

Here, ρ is the mass density and $\boldsymbol{u}$ is the bulk velocity of the plasma. $\boldsymbol{B}$ is the magnetic field due to both external currents and induced currents within the plasma. Under this set of equations, the "frozen-in" condition is strictly maintained.

It should be noted that the above equations are mainly valid for plasmas of high enough collisionality to maintain Maxwellian velocity distributions but low enough to approximate an infinitely conductive medium. Typically, the collision time-scale within the plume is longer than that needed to produce Maxwellian particle distributions. Therefore, although a fairly accurate portrayal of the field evolution may be obtained from Eqs. (1-4), the flow parameters may depart significantly from reality.

B. Non-Dimensionalization

Physical insight may be gained by non-dimensionalizing Eqs. (1-4) with respect to conditions present at the throat of the nozzle. Letting the subscript zero denote conditions at the throat, we define the following non-dimensional parameters: $\bar{\rho} = \rho/\rho_0$, $\bar{\boldsymbol{u}} = \boldsymbol{u}/u_0$, $\bar{\boldsymbol{B}} = \boldsymbol{B}/B_0$, $\bar{\boldsymbol{\nabla}} = L\boldsymbol{\nabla}$, $\tau = t/L/u_0$. Here, L is the scale length of the plasma. Eq. (1) thus becomes

$$\bar{\rho} \frac{\partial \bar{\boldsymbol{u}}}{\partial \tau} + \bar{\rho} \left(\bar{\boldsymbol{u}} \cdot \bar{\boldsymbol{\nabla}} \right) \bar{\boldsymbol{u}} = -\frac{1}{\beta_0} \bar{\boldsymbol{B}} \times \left(\bar{\boldsymbol{\nabla}} \times \bar{\boldsymbol{B}} \right), \tag{5}$$

where

$$\beta_0 = \frac{\rho_0 u_0^2}{B_0^2/\mu_0} \tag{6}$$

is the ratio of the kinetic energy density of the plasma flow to the energy density of the magnetic field at the nozzle throat.

It is evident from Eq. (5) that as β_0 increases, the plasma flow is less influenced by the presence of the magnetic field. Rather, the magnetic field is more influenced by the energetic plasma flow. Furthermore, plasma entering the throat further from the nozzle axis will experience large field gradients, therefore it may be expected that the divergence angle of the plume will depend on β_0 and the ratio of the plasma radius to the magnetic coil radius at the throat, which we will refer to as $\bar{r}_{p0}$.

C. Coordinate and Variable Transformations

We begin by describing the magnetic field in terms of its strength, B, and orientation, θ, with respect to the nozzle axis. Furthermore, because the magnetic field is axisymmetric, it is more convenient to describe it in terms of a flux function $\Phi(r, z, t)$.[7] Transforming each component yields

$$B_r = B \sin \theta = -\frac{1}{r} \left(\frac{\partial \Phi}{\partial z} \right)_r, \tag{7}$$

$$B_z = B \cos \theta = \frac{1}{r} \left(\frac{\partial \Phi}{\partial r} \right)_z. \tag{8}$$

Here, the subscript indicates which variable is held constant.

As a result, partial derivatives with respect to cylindrical coordinates must also be transformed. For a given parameter α, these transformations take the following form:

$$\left(\frac{\partial \alpha}{\partial r}\right)_z = \left(\frac{\partial \alpha}{\partial \Phi}\right)_z \left(\frac{\partial \Phi}{\partial r}\right)_z = rB\cos\theta \left(\frac{\partial \alpha}{\partial \Phi}\right)_z \tag{9}$$

$$\left(\frac{\partial \alpha}{\partial z}\right)_r = \left(\frac{\partial \alpha}{\partial z}\right)_\Phi + \left(\frac{\partial \alpha}{\partial \Phi}\right)_z \left(\frac{\partial \Phi}{\partial z}\right)_r = \left(\frac{\partial \alpha}{\partial z}\right)_\Phi - rB\sin\theta \left(\frac{\partial \alpha}{\partial \Phi}\right)_z. \tag{10}$$

If the velocity is expressed in terms of its component along the magnetic field line ($u_\parallel$) and that perpendicular to the magnetic field line ($u_\perp$), we may rewrite Eq.(3) in the following form:

$$B\frac{\partial \theta}{\partial t} = -\cos\theta \left(\frac{\partial u_\perp B}{\partial z}\right)_\Phi - \frac{u_\perp B\sin\theta}{r}, \tag{11}$$

$$\frac{\partial B}{\partial t} = -\sin\theta \left(\frac{\partial u_\perp B}{\partial z}\right)_\Phi + rB\left(\frac{\partial u_\perp B}{\partial \Phi}\right)_z + \frac{u_\perp B}{r}\cos\theta. \tag{12}$$

Eqs. (11) and (12) represent the time evolution of the magnetic field orientation and strength within the plasma due to flow perpendicular to the magnetic field lines. In other words, the "frozen-in" condition of ideal MHD dictates that elements of the plasma remain tied to lines of constant magnetic flux. If a plasma element has a velocity component perpendicular to this line, the line gets dragged along with the flow; impeding the motion of the plasma in return.

III.   Divergence Angle Scaling

The angle at which the exhaust plume emerges from a magnetic nozzle will largely determine the efficiency of the nozzle for propulsion applications. Defining the nozzle efficiency, η, as the ratio of the axial momentum flux emerging from the nozzle to that at the throat, it may be shown that this efficiency scales for small divergence angles as[7]

$$\eta \sim 1 - \theta_{div}^2/4, \tag{13}$$

where θ_{div} is the half angle at which the plume escapes the nozzle.

The divergence angle may be found by solving Eqs.(1-2) and (11-12) self-consistently, however, the complexity of these equations along with their time-dependent boundary conditions does not easily lend itself to a solution. Furthermore, any attempt at solving the steady-state form of these equations requires an assumption as to the boundary conditions, and thus the divergence angle itself. Rather, we assume that when steady state is reached, the plume would have reached far enough distance from the throat that the thruster can be considered a point source of plasma, and therefore the form of the plume would ultimately approximate that of a field-aligned, conical plasma flow with a half-angle given by θ_{div}. We then use a scaling relation for $u_\perp$ obtained from Eq.(1) to solve Eq.(11) for the parameters β_0 and $\bar{r}_{p0}$ necessary to arrive at θ_{div} in the limit as $t \to \infty$ and $z \to \infty$. The divergence angle is given by

$$\theta_{div} = \lim_{t,z\to\infty} \theta(z, \Phi_p, t), \tag{14}$$

with Φ_p describing the flux line corresponding to the radius of the plasma at the nozzle throat.

A.   Non-Dimensional Induction Equation

First, we cast Eq.(11) in non-dimensional form by normalizing each parameter according to section IIB. We will assume the nozzle's vacuum field can be approximated by the magnetic field of a single current loop, and use the radius of the loop, r_c, as the scale length. Eq.(11) may then be written as

$$\frac{\partial \theta}{\partial \tau} = -\cos\theta \left(\frac{\partial \bar{u}}{\partial \bar{z}}\right)_\Phi - \bar{u}\cos\theta \left(\frac{\partial \ln \bar{B}}{\partial \bar{z}}\right)_\Phi - \frac{\bar{u}}{\bar{r}}\sin\theta. \tag{15}$$

Here, $\bar{z} = z/r_c$ and $\bar{r} = r/r_c$ are the normalized axial and radial coordinates, respectively.

B. Perpendicular Velocity Scaling

A scaling relation for the velocity component perpendicular to the magnetic field lines may be obtained from the momentum equation. Using Eq.(1), we see that the perpendicular velocity scales as

$$\rho\frac{du_\perp}{dt} \sim -\frac{1}{\mu_0}\frac{B\delta B}{l}. \tag{16}$$

where δB is the change in magnetic field over the characteristic length l due to the plasma flow. This change scales according to Eq.(3), or

$$\frac{\delta B}{t} \sim \frac{u_\perp B}{l}. \tag{17}$$

Substitution of Eq.(17) into Eq.(16) and integration yields the following scaling relation for $u_\perp$

$$u_\perp \sim \exp\left(\frac{-B^2/\mu_0}{2\rho}\frac{t^2}{l^2}\right). \tag{18}$$

Using these relations and the requirement that $u_\perp$ vanish on axis ($\theta = 0$), we assume the following form for the non-dimensional perpendicular velocity in terms of normalized variables

$$\bar{u}_\perp = \sin\theta \exp\left(-\frac{u^2\tau^2}{2\beta\bar{l}^2}\right) H(\tau - \bar{z}), \tag{19}$$

with $\bar{l} = l/r_c$ and $\beta = \rho u^2/(B^2/\mu_0)$. The Heaviside step function, $H(\tau - \bar{z})$, appears because the plasma propagates at a finite speed. We assume the plasma front is at the nozzle throat at $\tau = 0$ and the prorogation speed is nearly constant ($u_z \sim u_0$, or $\bar{u} \sim 1$). This assumption seems to be justified by Mach probe measurements presented in Ref.[11].

C. Quasi-One-Dimensional Formulation

The evolution of the magnetic field orientation at each point in the flow is described by Eq.(15). Because we are interested in the ultimate divergence angle of the outermost flux surface, we are able to express the right hand side of this equation in a quasi-one-dimensional form dependent only on τ and $\bar{z}$ for a given Φ_p.

First, we realize that the scale length over which the magnetic field changes for a plasma element within the plume will mostly depend on the radial position of the element at the throat. For the plasma edge, we may write this scale length as $\bar{l} = 1/\bar{\kappa}_0(\bar{r}_{p0})$, where $\bar{\kappa}_{p0}$ is the dimensionless flux line curvature at the normalized radius of the plasma . In other words, plasma injected into the nozzle throat at a larger percentage of the coil radius will see a flux line of larger curvature than plasma injected closer to the axis. As a result, the magnetic field will vary over a smaller scale length for plasma elements further from the nozzle centerline.

Additionally, β will vary within the plume due to gradients in the plasma density and magnetic field strength. Modeling the plume as a conical plasma with a half-angle given by θ_{div},[7] it is possible to show that the axial variation of β along Φ_p far from the nozzle throat can be approximated by the following expression:

$$\beta(\bar{z}) = \beta_0 \frac{\bar{z}^2}{\bar{r}_{p0}^2}\tan^2\theta_{div}\sec^4\theta_{div}. \tag{20}$$

Assuming the magnitude of the plasma velocity does not change significantly in the plume ($v \sim 1$), Eq.(19) may be rewritten as

$$\bar{u}_\perp = \sin\theta \exp\left(-\frac{\Gamma^2\tau^2}{\bar{z}^2}\right) H(\tau - \bar{z}), \tag{21}$$

where

$$\Gamma = \frac{\bar{\kappa}_{p0}\bar{r}_{p0}\cos^2\theta_{div}}{\sqrt{2\beta_0}\tan\theta_{div}} \tag{22}$$

is a function only of β_0, $\bar{r}_{p0}$, and θ_{div}.

With the first term on the right hand side of Eq.(15) known, we now turn our attention to the second and third terms. Apparently, the derivative of the natural logarithm of the magnetic field strength will always be inversely proportional to axial distance. The constant of proportionality will depend on the flux surface

on which this derivative is taken and the form of the magnetic field. For example, on the nozzle axis, this term scales as $-3/\bar{z}$ and $-2/\bar{z}$ for a dipole field and conical field, respectively. Off axis, the constant of proportionality will decrease. We may then assume the following

$$\left(\frac{\partial \ln \bar{B}}{\partial \bar{z}}\right)_{\Phi} \sim \frac{a_1(\tau, \Phi_p)}{\bar{z}}, \tag{23}$$

Here, a_1 is a number that will typically lie within the range $\{-3, -2\}$ because the magnetic field is assumed to transition from that of a single current loop to a conical structure.

Similarly, the third term on the right hand side of Eq.(15) is approximately inversely proportional to axial distance. Taking advantage of the conical plasma assumption, the radial distance along the outermost flux surface far from the nozzle goes as $\bar{r} \sim \bar{z} \tan \theta_{div}$. This term may then be expressed as

$$\frac{\bar{u}_\perp}{\bar{r}} \sin \theta \sim \frac{\bar{u}_\perp}{\bar{z}} \frac{\sin \theta}{\tan \theta_{div}} \sim \frac{\bar{u}_\perp}{\bar{z}} \cos \theta \frac{\tan \theta}{\tan \theta_{div}} \sim a_2(\tau, \Phi_p, \bar{z}) \frac{\bar{u}_\perp}{\bar{z}} \cos \theta, \tag{24}$$

where the solution eventually shows that a_2 most commonly falls within the range $\{1, 4\}$ for $\theta_{div} \leq 90^o$.

D. Curvature Expression

It is not possible to find an explicit expression for the flux function describing the magnetic field of a single current loop because the field components are non-integrable. However, the geometry of the field near the nozzle throat allows the normalized radius of curvature to be estimated from

$$\bar{\mathcal{R}}_0 = \lim_{\bar{z}\to 0} \bar{z} \left[1 + (B_r/B_z)^{-2}\right]^{1/2}. \tag{25}$$

Substitution of B_r and B_z for a single current loop yields the following expression for the normalized curvature ($\bar{\kappa}_{p0} = 1/\bar{\mathcal{R}}_0$) of the flux line corresponding to the plasma radius at the nozzle throat:

$$\bar{\kappa}_{p0} = \frac{\bar{r}_{p0}}{1 - \bar{r}_{p0}}. \tag{26}$$

As expected, the curvature is zero along the nozzle axis ($\bar{r} = 0$) and infinite towards the nozzle radius ($\bar{r} = 1$).

E. θ-Evolution

Substitution of Eqs.(21), (23), and (24) into Eq.(15) yields the following expression for the evolution of the magnetic field orientation along the plasma edge ($\theta_p = \theta(z, \Phi_p, t)$):

$$\frac{\partial \theta_p}{\partial \tau} = -\left(\frac{2\Gamma^2 \tau^2}{\bar{z}^3} + \frac{a_3}{\bar{z}}\right) \bar{u}_\perp \cos \theta_p, \tag{27}$$

where $a_3 = a_1 + a_2$. In essence, Eq.(27) describes how the vacuum magnetic field far from a magnetic nozzle changes from its initial orientation due to the arrival of a propagating plasma front of conical shape.

Direct integration of Eq.(27) is possible if we treat a_3 as a constant equivalent to its average over time ($\bar{a}_3 \approx \int_0^\infty a_3 d\tau$). Using this simplification, the orientation of the magnetic field of the outer flux line with respect to time may be approximated by

$$\frac{\tan \theta_p}{\tan \theta_p^*} = \exp\left\{-e^{-\Gamma^2} + \frac{\tau}{\bar{z}} e^{-\frac{\Gamma^2 \tau^2}{\bar{z}^2}} - (1 + \bar{a}_3) \frac{\sqrt{\pi}}{2\Gamma} \left[\text{erf}\left(\frac{\Gamma \tau^2}{\bar{z}^2}\right) - \text{erf}(\Gamma)\right]\right\}, \tag{28}$$

where θ_p^* is a constant resulting from the integration and represents the orientation of the magnetic field as the plasma arrives at $\bar{z}$. Finally, taking the limit of Eq.(26) as $\tau \to \infty$ yields

$$\frac{\tan \theta_{div}}{\tan \theta_p^*} = \exp\left\{-e^{-\Gamma^2} - (1 + \bar{a}_3) \frac{\sqrt{\pi}}{2\Gamma} [1 - \text{erf}(\Gamma)]\right\}. \tag{29}$$

The above expression is a transcendental equation for θ_{div} and depends on the dimensionless variables β_0 and $\bar{r}_{p0}$. Thus, if reasonable estimates for θ_p^* and $\bar{a}_3$ are known, the divergence angle may be found for a given β_0 and $\bar{r}_{p0}$.

F. Geometric Argument: θ_p^* Estimation

Expressions for θ_p^* and $\bar{a}_3$ are not immediately obvious from the formulation of the problem. θ_p^* will depend on the initial vacuum magnetic field, however, its value will also be influenced by currents within the plasma before the plasma front arrives. A careful study of the boundary conditions at the plasma front may yield a reasonable expression for θ_p^*, however, we instead use a geometric argument to estimate its value based on the initial plasma radius.
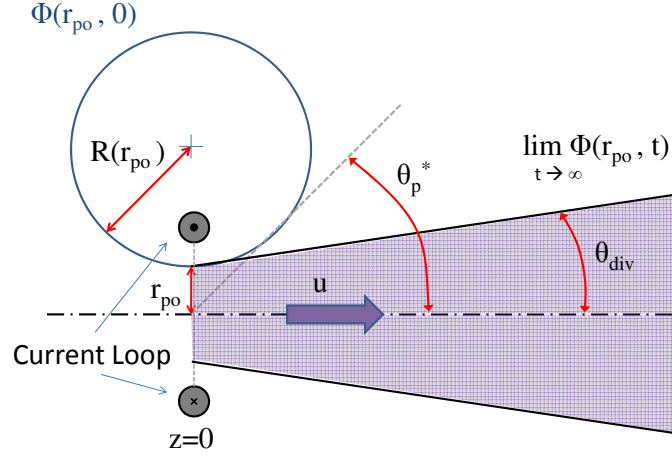
Figure 2. Diagram describing the definition of the initial magnetic field orientation at the plume edge, θ_p^*. Also shown is the geometry of the estimated flux line used to express θ_p^* in terms of $\bar{r}_{p0}$.

To simplify the problem, we treat the initial magnetic field orientation (θ_p^*) at the plume edge as a parameter dependent only upon the initial plasma radius and the initial magnetic field. This angle can be estimated as the angle made between the nozzle axis and a line connecting the origin to the tangent of the flux line corresponding to the plasma edge at $\tau = 0$ (fig. 2). Because an expression does not exist for the flux line of a single current loop magnetic field, we instead assume the flux line approximates a circle with radius given by the radius of curvature found in Section IIID. Solving for θ_p^* yields

$$\tan\theta_p^* = \frac{\bar{r}_{p0}}{1 - \bar{r}_{p0}}\sqrt{\bar{r}_{p0}^2 - 2\bar{r}_{p0} + 2}. \tag{30}$$

Therefore, as the plasma radius at the throat increases, the amount of work needed to arrive at a given angle of divergence also increases.

G. Divergence Angle Scaling

For the sake of simplicity, we also assume that the physical phenomena described by the last two terms in Eq.(15) cancel out on average ($\bar{a}_3 = 0$). As it turns out, the solution of Eq.(30) does not depend strongly on the value of $\bar{a}_3$, and only deviates by about 20% within the range $\{-1, 6\}$. However, for $\bar{a}_3 < -1$, the solution does not converge to a physically meaningful result. Further investigation is required to determine the significance of the two regimes.

We now have all of the information needed to solve Eq.(30) numerically for θ_{div}. Plots of this solution for different values of β_0 and $\bar{r}_{p0}$ may be seen in figure 3. It is clear from figure 3 that the divergence angle decreases both as β_0 increases and as $\bar{r}_{p0}$ decreases. Therefore, as expected, compact and energetic plasmas are most desirable for propulsion applications. Furthermore, it is evident that the divergence angle will depend more heavily upon $\bar{r}_{p0}$ than β_0. This is because $\bar{r}_{p0}$ determines the field gradients experienced by the plasma, the way β evolves within the plume, and the amount of work needed to bring the magnetic field orientation to its final value.

Also shown in figure 3 is a dashed line corresponding to an approximate shift from a region where the divergence angle varies strongly with β_0 to a region where it varies weakly with β_0. This line was qualitatively fitted to the graph and is characterized by the value

$$\beta_0^* \simeq 0.12 \bar{r}_{p0}^{1/2} \tag{31}$$

Figure 3 then suggests that large improvements in the nozzle efficiency can be seen as β_0 increases towards β_0^*. For $\beta_0 > \beta_0^*$, only minimal improvements are realized.
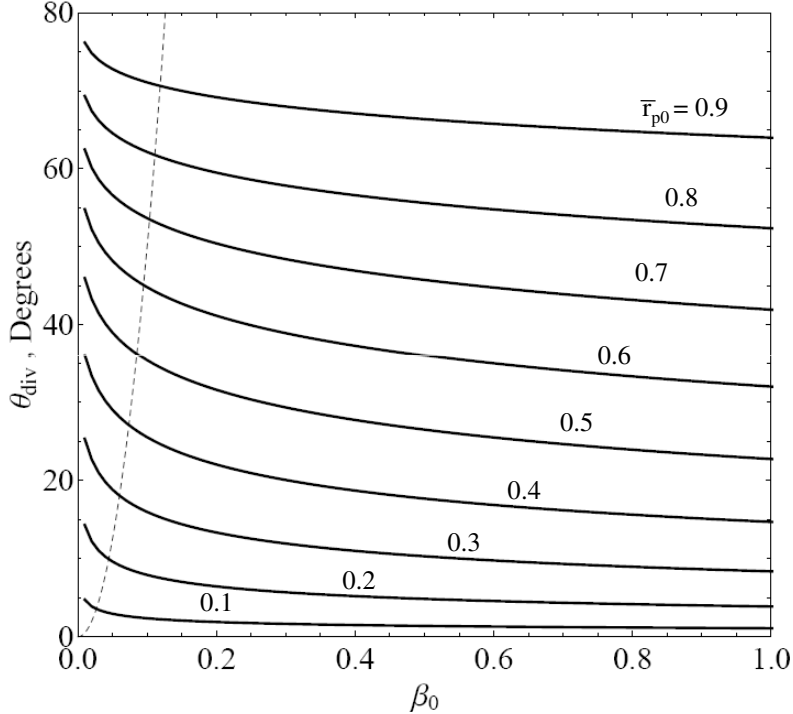

Figure 3. Divergence angle as a function of β_0 for different values of $\bar{r}_{p0}$ as obtained from Eq.(30). The dashed line qualitatively indicates a transition region between large divergence angle improvements and marginal improvements for increasing β_0.

IV. Discussion

A. Numerical Comparison: Divergence Angle

Numerical simulations presented by Breizman et al.[8] may be used to examine the validity of Eq.(30). In these simulations, the authors numerically solved for the steady-state solution of a cold uniform plasma expanding through the fringe field of a semi-infinite solenoid. Results for two different inlet conditions were presented: $(\bar{r}_{p0} = 0.60, \beta_0 = 0.56)$ and $(\bar{r}_{p0} = 0.40, \beta_0 = 0.56)$. The first case resulted in a divergence angle of approximately 45° with Eq.(30) predicting a divergence angle of 35°, while the second case gave approximately 30° with Eq.(30) predicting 17°. This quantitative discrepancy is most likely due to a combination of the simplifying assumptions related to $\bar{a}_3$ and θ_p^*.

Additionally, the paraxial magnetic field approximation used by the authors in Ref.[8] breaks down in the plume where $B_r \approx B_z$ for $\theta \approx 45^o$. This inconsistency could also explain the error between their numerical results and our analytical results, which do not employ the paraxial approximation. Further investigation is required to determine the exact source of this error.

B.   Experimental Comparison: Divergence Angle

Unfortunately, experimental validation of the above scaling relation for the divergence angle is limited due to a lack of applicable data presented in the literature thus far. However, data acquired from the Detachment Demonstration Experiment (DDEX)[13] in 2007 at NASA Marshall allows a comparison between Eq.(30) and experimentation.

The plasma flow presented in ref.[13] is characterized by the following non-dimensional parameters at the nozzle throat: $\bar{r}_{p0} \approx 0.04$, $\beta_0 \approx 0.07$. Measurements of the radial density profile along the nozzle axis indicate a divergence angle of $\theta_{div} \approx 15^o$. However, the divergence angle predicted by Eq.(3) for this flow is approximately 1°: a value significantly lower than that measured in the experiment.

The discrepancy between the measured and predicted divergence angle can most likely be explained by the thermal expansion of the plasma, which is not taken into account when deriving Eq.(30). The data in ref.[13] indicates the thermal energy density is nearly one-third the kinetic energy density at the nozzle throat. It may then be expected that adiabatic expansion of the plasma increases the divergence angle beyond predicted values. Additionally, the assumption that $\bar{a}_3 = 0$ decreases the expected divergence angle for a given β_0 and $\bar{r}_{p0}$. However, it was found that changing the value of $\bar{a}_3$ does not significantly alter the predicted divergence angle. More experimental comparisons are required to determine the specific cause of the discrepancy between experimental and predicted divergence angles.

V.   Conclusion

An expression is found for the divergence angle of a propulsive plasma flow emerging from a magnetic nozzle. As expected, the divergence angle decreases as the injected plasma becomes more compact and energetic with respect to the magnetic field of the nozzle. The results suggest a transition region exists where increasing the kinetic energy density at the nozzle throat only marginally improves the nozzle efficiency. However, further studies are required to validate the divergence angle expression with numerical and experimental results.

Acknowledgments

References

[1]Cohen, S., Siefert, N., and Stange, S., "Ion acceleration in plasmas emerging from a helicon-heated magnetic mirror device," *Physics of Plasmas*, Vol. 10, 2003, pp. 2593.

[2]Chang Diaz, F. R., "An overview of the VASIMR engine: High power space propulsion with RF plasma generation and heating," *AIP Conf. Proc.*, Vol. 595, 2001, pp. 3, 15.

[3]Gerwin, R. A., Marklin G. J., Sgro, A. G., and Glasser, A. H., *Characterization of plasma flow through magnetic nozzles*, Technical Report LA-UR-89-4212, Los Alamos National Laboratory, 1989.

[4]Moses, R. W., Gerwin, R. A., and Schoenberg, K. F., "Resistive Plasma Detachment in Nozzle Based Coaxial Thrusters," *AIP Conf. Proc.*, Vol. 246, 1992, pp. 1293.

[5]Hooper, E. B., "Plasma Detachment from a Magnetic Nozzle," *Journal of Propulsion and Power*, Vol. 9, 1993, pp. 757.

[6]Schmit, P. F. and Fisch, N. J., "Magnetic detachment and plume control in escaping magnetized plasma," *J. Plasma Physics*, Vol. 75, 2009, pp., 359, 371.

[7]Arefiev, A. V. and Breizman, B. N., "Magnetohydrodynamic scenario of plasma detachment in a magnetic nozzle," *Physics of Plasmas*, Vol. 12, 2005.

[8]Breizman, B. N., Tushentsov, M. R., and Arefiev, A. V., "Magnetic nozzle and plasma detachment model for a steady-state flow," *Physics of Plasmas*, Vol. 15, 2008.

[9]Winglee, R., Ziemba, T., Giersch, L., Prager, J., Carscadden, J., and Roberson, B. R., "Simulation and laboratory validation of magnetic nozzle effects for the high power helicon thruster," *Physics of Plasmas*, Vol. 14, 2007.

[10]Ilin, A. V., Chang-Diaz, F. R., Squire, J. P., Tarditi, A. G., Breizman, B. N., and Carter, M. D., "Simulations of Plasma Detachment in VASIMR," *40th AIAA Aerospace Sciences Meeting*, Reno, NV, Jan. 1993. AIAA Paper 93-0817.

[11]Deline, C. A., Bengston, R. D., Breizman, B.N., Tushentov, M. R., Jones, J. E., Chavers, D. G., Dobson, C. C., and Schuettpelz, B. M., "Plume detachment from a magnetic nozzle," *Physics of Plasmas*, Vol. 16, 2009.

[12]Chancery, W., "Investigation of Plasma Detachment from a Magnetic Nozzle," M.S. Thesis, Aerospace Engineering Dept., Auburn Univ., Auburn, AL, 2007.

[13]Freidberg, J. P., *Ideal Magnetohydrodynamics*, 1st ed., Springer, New York, 1987, Chaps. 1, 3.